RSC Advances

ROYAL SOCIETY OF CHEMISTRY

www.rsc.org/advances

Four cobalt(II) coordination polymers with diverse topologies derived from flexible bis(benzimidazole) and aromatic dicarboxylic acids：Syntheses, crystal structures and catalytic properties

Xiao Xiao Wang[a], Baoyi Yu[b], Kristof Van Hecke[b], Guang Hua Cui*[a]

[a]*College of Chemical Engineering, Hebei United University, 46 West Xinhua Road, Tangshan 063009, Hebei, PR China.*

[b]*Department of Inorganic and Physical Chemistry, Ghent University, Krijgslaan 281 S3, B-9000 Ghent, Belgium*

*Corresponding author. E-mail: tscghua@126.com

Submitted **to *RSC Advances***

ABSTRACT

Four mixed ligand coordination polymers based on the flexible bis(5,6-dimethybenzimidazole) and aromatic dicarboxylic acids, namely, $[Co(L1)(bpdc)]_n$ (**1**), $\{[Co(L1)(npht)]\cdot 0.5H_2O\}_n$ (**2**), $[Co(L2)(bpdc)]_n$ (**3**), and $[Co(L3)(bpdc)(H_2O)]_n$ (**4**) (L1 = 1,4-bis(5,6-dimethylbenzimidazol-1-ylmethyl)benzene, H_2bpdc = 4,4'-biphenyldicarboxylic acid, L2 = 1,3-bis(5,6-dimethylbenzimidazol-1-ylmethyl)benzene, H_2npht = 3-nitrophthalic acid, L3 = 1,1'-bis(5,6-dimethylbenzimidazole)methane) have been hydrothermally synthesized and structurally characterized. Polymer **1** features a 3D three-fold interpenetrating **dia** array with 4-connected 6^6 network, while **2** exhibits a 3D noninterpenetrated 3-connected framework with 10^3-**ThSi$_2$** architecture. **3** and **4** have two-dimensional 3-connected (6^3) and 4-connected ($4^4.6^2$) topologies, respectively. Complex **4** ultimately is extended into an unusual 3D (3,5)-connected **seh**-3,5-P21/c supramolecular network *via* O–H···O hydrogen bonding interactions. The fluorescence and catalytic properties of the complexes for the degradation of the Congo red azo dye in a Fenton-like process are reported.

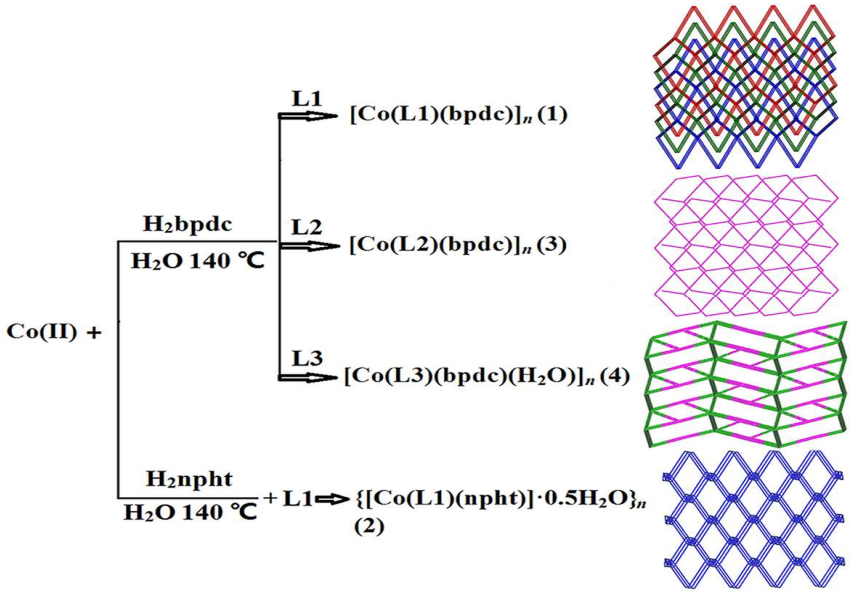

Introduction

The rational design and synthesis of metal-organic frameworks (MOFs) have received much attention not only because of the intriguing variety of topologies structures but also due to their potential applications in catalysis, luminescence, gas storage, ion exchange, magnetism, and so on.[1,2] Generally, the generation of novel coordination polymers is greatly influenced by factors such as the coordination nature of metal ions, flexibility, spacer length and steric hindrance of the ligands, the metal/ligand ratio, solvent, possible counter-ions and non-covalent interactions (such as H-bonding and π–π stacking). However, it still remains a long-term challenge on modifying the building blocks and controlling the assembled motifs for obtaining the required products. Hence, systematic research on this topic is crucial in understanding how these factors affect the metal coordination framework for the rational design of crystalline materials so as to conform to the coordination preferences of the metal. In recent years, flexible bis(benzimidazole) ligands have attracted much attention and have been used as classic N-containing ligands, in which the sp^3 hybridization of $–CH_2–$ spacers allows them to bend and rotate when coordinating to metal centers and consequently generate more robust and intricate networks such as ($6^5.8$) **msw/*P*42/*nnm*** and **mok** topology, interpenetrating networks.[3,4] Among the series of benzimidazole derivatives, the most prominent compound is 5,6–dimethylbenzimidazole, which serves as an axial ligand for the cobalt center in coenzyme B_{12}.[5] Bis(5,6-dimethylbenzimidazole) as bridging ligand, which participates in the construction of coordination polymers, can provide more information for us to investigate the influence of methyl substituted derivatives of the benzimidazole on the structures and properties of the resulting architecture.[6] Moreover, to the best of our knowledge, such metal coordination polymers based on the flexible bis(5,6-dimethylbenzimidazole) and 4,4'-biphenyldicarboxylic acid (H_2bpdc)/3-nitrophthalic acid (H_2npht) ligands have only been scarcely reported.[7] In our efforts to systematically investigate the effects of the spacer length of flexible bis(5,6-dimethylbenzimidazole) ligands and other factors on the structures of Co(II) complexes mixed with aromatic dicarboxylic acid, four new coordination polymers have been hydrothermally synthesized and characterized, formulated as $[Co(L1)(bpdc)]_n$ (**1**), $\{[Co(L1)(npht)]\cdot 0.5H_2O\}_n$ (**2**), $[Co(L2)(bpdc)]_n$ (**3**), and $[Co(L3)(bpdc)(H_2O)]_n$ (**4**) (L1 = 1,4-bis(5,6-dimethylbenzimidazol-1-ylmethyl)benzene, H_2bpdc = 4,4'-biphenyldicarboxylic acid, L2 = 1,3-bis(5,6-dimethylbenzimidazol-1-ylmethyl)benzene, H_2npht = 3-nitrophthalic acid, L3 =

1,1'-bis(5,6-dimethylbenzimidazole)methane). The crystal structures and topological analyses of these polymers, along with a systematic investigation of the effect of the spacer length of flexible bis(5,6-dimethylbenzimidazole) ligands on the ultimate frameworks, is presented and discussed. In addition, the thermal stabilities, fluorescence properties and catalytic properties of **1**-**4** for the degradation of Congo red in a Fenton-like process are investigated.

Experimental details

Materials and general methods

All reagents and solvents were obtained from commercial sources and used without further purification. The ligands were synthesized according to the literature procedure.[8] Elemental analysis (C, H, and N) was performed on a Perkin-Elmer 240C Elemental Analyzer. IR spectra were recorded from KBr pellets in the range of 4000−400 cm^{-1} on an Avatar 360 (Nicolet) spectrophotometer. Thermogravimetric analysis (TGA) was carried out on a NETZSCH TG 209 thermal analyzer from room temperature to 800 °C with a heating rate of 10 °C/min under N_2 atmosphere. Luminescence spectra for the powdered solid samples were measured at room temperature on a Hitachi F-7000 fluorescence spectrophotometer. X-ray powder diffraction (PXRD) measurements were made on a Rigaku D/Max-2500PC X-ray diffractometer using Cu-Kα radiation (λ = 0.1542 nm) and ω-2θ scan mode at 293 K.

Synthesis of complexes 1-4

$[Co(L1)(bpdc)]_n$ 1. A mixture of $CoCl_2 \cdot 6H_2O$ (23.8 mg, 0.1 mmol), L1 (39.4 mg, 0.1 mmol), H_2bpdc (24.2 mg, 0.1 mmol), NaOH (4.0 mg, 0.1 mmol) and 10 mL water was heated at 140 °C for 3 days in a Teflon-lined vessel (25 mL). After, the mixture was cooled to room temperature at a rate of 5 °C/h. Pink block crystals suitable for single-crystal X-ray diffraction were obtained by filtration. Yield: 40% (based on $CoCl_2 \cdot 6H_2O$). Calcd for $C_{40}H_{34}CoN_4O_4$ (693.64): C 69.26, H 4.94, N 8.08; found: C 69.50, H 4.79, N 8.30. IR (KBr, cm^{-1}): 3101(m), 2923(w), 1601(s), 1524(m), 1369(s), 1230(w), 1011(w), 840(m), 768(m), 689(m), 580(w), 443(m).

$\{[Co(L1)(npht)] \cdot 0.5H_2O\}_n$ 2. Complex **2** was prepared in the same way as that for **1**, except using H_2npht (21.1 mg, 0.1 mmol) instead of H_2bpdc (24.2 mg, 0.1 mmol). Purple block crystals of complex **2** suitable for single-crystal X-ray diffraction were acquired. Yield: 53% (based on $CoCl_2 \cdot 6H_2O$). Calcd for $C_{34}H_{32}CoN_5O_{7.50}$ (689.58): C 59.22, H 4.68, N 10.16; found: C 59.40, H 4.49, N 10.30. IR (KBr, cm^{-1}): 3417(s), 2923(w), 2366(m), 1624(m), 1534(m), 1392(w), 1340(w),

1133(s), 662(w), 526(w), 471(m).

[Co(L2)(bpdc)]$_n$ 3. Complex **3** was obtained by a similar procedure of **1**, except that L2 (39.4 mg, 0.1 mmol) was used instead of L1. Purple block-like crystals of **3**, suitable for X-ray diffraction, were acquired at a yield of 48% based on $CoCl_2 \cdot 6H_2O$. Calcd for $C_{40}H_{34}CoN_4O_4$ (693.64): C 69.26, H 4.94, N 8.08; found: C 69.40, H 4.79, N 8.20. IR (KBr, cm^{-1}): 2923(w), 2372(w), 1670(w), 1598(m), 1515(m), 1406(s), 1105(m), 851(m), 766(m), 684(w), 465(m).

[Co(L3)(bpdc)(H$_2$O)]$_n$ 4. Complex **4** was prepared by following the procedure depicted for **1**, but using L3 (30.4 mg, 0.1 mmol) instead of L1. Pink block crystals of **4**, suitable for X-ray diffraction, were acquired at a yield of 59% based on $CoCl_2 \cdot 6H_2O$. Calcd for $C_{33}H_{30}CoN_4O_5$ (621.54): C 63.77, H 4.86, N 9.01; found: C 63.60, H 4.79, N 9.23. IR (KBr, cm^{-1}): 3410(m), 3120(w), 2997(w), 1619(m), 1554(m), 1515(m), 1431(m), 1393(s), 1199(w), 819(m), 748(m), 722(m), 632(w), 426(w).

X-ray crystallography

Crystallographic data for complexes **1-4** were collected on a Bruker Smart CCD diffractometer with Mo Kα radiation (λ = 0.71073 Å) by using an ω-2θ scan mode. Semi-empirical absorption corrections were applied using the SADABS program.[9] The structures were solved by direct methods and refined on F^2 by full-matrix least-squares using the SHELXL-97 program package.[10] All non-hydrogen atoms were refined anisotropically. The hydrogen atoms of all water molecules could be located from a difference Fourier map, while the other hydrogen atoms were included in calculated positions and refined with isotropic thermal parameters riding on the corresponding parent atoms. Complex **2** showed disorder in carboxy group C35, O5, O6 of npht ligand; these atoms were refined with a split model with site occupation factor 0.50, DFIX for restraining distances with related disordered atoms(C–C = 1.5$\pm$0.01, C–O = 1.25$\pm$0.02 Å). Crystallographic data and structure determination statistics are listed in Table 1, and selected bond lengths and angles for the complexes are listed in Table S1.

(Insert Table 1)

Results and discussion

Synthesis of the Polymers

The hydrothermal method has been extensively explored as an effective and powerful tool in

the self-assembly of MOFs. In addition, it is well-known that the Co(II) ion is able to coordinate simultaneously in solution to both oxygen- and nitrogen-containing ligands.[11] So the cobalt metal salt was used to synthesize intriguing frameworks based on the mixed-ligands of distinct aromatic dicarboxylic acids and flexible bis(5,6-dimethylbenzimidazole) by hydrothermal method. By varying the molar ratio/composition of the initial reactants, reaction time or temperature, the single crystals of **1**-**4** suitable for single-crystal X-ray diffraction analysis were successfully obtained. The results of elemental analysis for the complexes were in good agreement with the theoretical requirements of their compositions (from the results of X-ray structural analysis).

Crystal structure of $[Co(L1)(bpdc)]_n$ (1)

The X-ray crystallographic study shows that complex **1** crystallizes in the monoclinic space group *C*2/*c*. There are one half of a Co atom, one half of an L1 and one half of a $bpdc^{2-}$ ligand in the asymmetric unit of complex **1**. As shown in Fig. 1a, the central Co atom is four-coordinated by two nitrogen atoms from two L1 ligands and two oxygen atoms originating from two distinct $bpdc^{2-}$ ligands to give a distorted tetrahedral geometry with the τ parameter being 0.83.[12] The Co–N bond lengths are 2.034 (18) Å and the Co–O ones are 1.937(15) Å, which are in the normal range of those observed in cobalt complexes.[13]

In **1**, each $bpdc^{2-}$ anion displays a bisbridging/bis(monodentate) coordination mode linking neighboring Co(II) ions to generate a neutral 1D zigzag $[Co(bpdc)]_n$ chain along the *c*-axis with a through-ligand Co···Co distance of 15.196 (9) Å and a Co–Co–Co angle through the bpdc anions of 120.22(1)°. Each L1 ligand acts as a μ_2-bridging linker with two benzimidazole rings being in a parallel fashion. The 1D infinite chain (Co(II)/L1 chain) along the *b*-axis is formed by the *anti*-conformational L1 ligands and Co(II) ions with a Co···Co separation of 14.387(12) Å. The interlaced connection of the 1D chains of Co(II)/$bpdc^{2-}$ and Co(II)/L1 gives rise to the 3D framework by sharing Co(II) ions in **1** (Fig. 1b). A topological analysis of this network was performed with the TOPOS 4.0 software.[14] In complex **1**, the Co atom connecting four neighboring Co atoms can be considered as 4-connected node, the L1 and $bpdc^{2-}$ bridging ligands can be regarded as linkers, hence the 3D structure can be classified as a **dia** topology with point symbol 6^6. In order to avoid an extremely large void space, **1** exhibits a 3-fold interpenetrating structure (Fig. 1c). The three interpenetrated nets are related by a single translational vector (Class Ia),[15] with $Z_t = 3$ and $Z_n = 1$, where Z_t represents the number of interpenetrated nets related by

translation and Z_n denotes the number of interpenetrated nets related by crystallographic symmetry.[16] Moreover, the 3D supramolecular framework is further stability by the π-π interactions between neighbouring benzene rings from L1 and $bpdc^{2-}$ ligands with the center-to-center separations of 3.744(2) Å. Intriguingly, a void volume of 327 $Å^3$ is also left after interpenetration and the pore volume ratio was calculated to be 9.1% by the PLATON program.[17]

(Insert Fig. 1)

Crystal structure of $\{[Co(L1)(npht)]\cdot 0.5H_2O\}_n$ (2)

X-ray single crystal structure analysis reveals that **2** features a 3D MOF in which the asymmetric unit contains one Co atom, two half of L1 ligands, one $npht^{2-}$ ligand and half a lattice water molecule. As shown in Fig. 2a, the Co center exhibits a trigonal bipyramidal environment with two nitrogen atoms (N1, N3) deriving from benzimidazolyl of two different L1 ligands and three oxygen atoms (O4, O5A, O6, symmetry code: A: -*x*+3/2, -*y*+3/2, -*z*+1) originating from two different $npht^{2-}$ anions. The Co–N distances are 2.025(3) and 2.048(3) Å, and the Co–O lengths are in the range of 1.924(3)-2.281(5) Å. The bond angles at the Co center range from 71.20(2) to 72.78(16)°.

In complex **2**, each fully deprotonated $npht^{2-}$ ligand connected with two Co atoms *via* its carboxylate groups adopts a tridentate bridging μ_2-η^1:η^2 coordination fashion, resulting in a dinuclear $[Co_2(npht)_2]$ unit with a non-bonding Co···Co separation of 4.621(8) Å (Fig. 2b). Two bidentate bridging, crystallographically independent, L1 ligands (*L1-1*, denoted by N1–N2; *L1-2*, denoted by N3–N4) interlaced connect to give rise to the 3D framework by sharing Co(II) ions in **2** (Fig. 2c), wherein each Co atom is bound to two symmetrical Co atoms through *L1-1* and to two other symmetrical Co atoms through *L1-2*. The Co–Co distances through *L1-1* and *L1-2* are 12.786(14) and 11.809(15) Å, respectively. Differences observed in Co–Co distances through the L1 ligands can be attributed to the diversity of the torsion angles between the benzimidazole rings (180(14)° in *L1-1* and 59.73(16)° in *L1-2*). In the topology view, the two types of ligands act as connectors, each Co is linked to three other Co atoms and this can be considered as a three-connected node. The 3D framework of **2** can be represented to be a uninodal 3-connected **$ThSi_2$** topology with the Schläfli symbol (10^3), as displayed in Fig. 2d. Interestingly, calculations from the X-ray structure data show that the framework possesses a solvent-accessible volume of

231.2 Å^3, corresponding to 3.6% of the unit cell.

(Insert Fig. 2)

Crystal structure of [Co(L2)(bpdc)]$_n$ (3)

Complex **3** exhibits a 2D network and crystallizes in the orthorhombic space group *pbca*. The asymmetric unit of **3** consists of one Co center, one L2 and one bpdc^{2-} ligand. The coordination geometry of the Co(II) ion is a distorted octahedron. Each Co(II) ion is connected to four oxygen atoms from two bpdc^{2-} ligands with the Co–O bond distance ranging from 2.104(4) to 2.237(4) Å, and two nitrogen atoms from two L2 ligands with bond lengths of Co–N of 2.072(4) and 2.082(4) Å (Fig. 3a). The best equatorial plane is formed by two bidentate chelating bpdc^{2-} carboxylate oxygen atom (O1, O2, O4B, symmetry code: B: -*x*+3/2, *y*+1/2, *z*) and one nitrogen atom (N3A, symmetry code: A: -*x*, -*y*+1, -*z*+1) from L2 ligands, the axial positions are occupied by O3B and N1 atoms. The Co center is approximately coplanar with the mean plane of the four equatorial atoms with a deviation of 0.155 Å.

Each L2 ligand exhibits the *anti*-conformation with the dihedral angle between two benzimidazole planes of 87.95(2)°, and acts as a μ_2-bridging linker bridging adjacent Co atoms to assemble into a dinuclear [Co$_2$(L2)$_2$] unit. The Co···Co distances through L2 ligands are 10.337(13) Å. Notably, both carboxylate groups of bpdc^{2-} ligands show the bidentate chelating coordination mode and further crosslink the [Co$_2$(L2)$_2$] units to form a 2D grid layer by sharing Co(II) ions in **3** (Fig. 3b). From the viewpoint of structural topology, the L2 and bpdc^{2-} ligands act as connectors, hence the structure of complex **3** can be considered as a 2D uninodal 3-connected **hcb** topology with a point symbol of (6^3) (Fig. 3c). The solvent-accessible volume is 710 Å^3 per unit cell and the pore volume ratio was calculated to be 9.9%.

(Insert Fig. 3)

Crystal structure of [Co(L3)(bpdc)(H$_2$O)]$_n$ (4)

The asymmetric unit of **4** contains one cobalt atom, one L3 ligand, one bpdc^{2-} ligand and one coordinated water molecule. As shown in Fig. 4a, the Co(II) center shows a distorted octahedral coordination geometry, and is coordinated by two nitrogen atoms from two L3 ligands, three oxygen atoms from two distinct bpdc^{2-} ligands and one oxygen atom from the coordinated water molecule. The Co–O bond distances vary from 2.021(2) to 2.247(2) Å, the Co–N1, Co–N4B

(symmetry code: B: -*x*+2, *y*-1/2, -*z*+1/2) bond lengths are 2.210(3) and 2.097(3) Å, respectively. The bond angles at the Co center range from 60.48(8) to 177.22(9)°.

The fully deprotonated $bpdc^{2-}$ ligands coordinate to neighboring Co atom acting in a μ_2-η^2:η^1 coordination mode to form neutral one-dimensional (1D) zigzag $[Co(bpdc)]_n$ chains traveling along the crystallographic *c*-direction with a through-ligand Co–Co contact distance of 15.121(16) Å. The Co–Co–Co angle through the bpdc anions is 145.87(4)°. Furthermore, the $[Co(bpdc)]_n$ chains are conjoined into 2D flat (4,4) rhomboid grid-like layers running parallel to the *bc* crystal plane through the linking of L3 ligands with a through-ligand Co–Co distance of 10.011(10) Å (Fig. 4b). The L3 ligands adopt an *anti*-conformation in which the dihedral angle between the mean plane of two benzimidazole rings is 87.16(6)°. The dimensions of the intralayer incipient voids are 10.01 × 15.12 Å, as measured by through-space Co–Co distances. From the topological view, the Co center can be considered as a 4-connected node, the two types of ligands act as linkers. As a result, the 2D layer of **4** displays a uninodal 4-connected **sql** net and with a point symbol of $(4^4.6^2)$. The 2D layers are further interlinked *via* H-bonds between the water ligands and bidentate chelating carboxylate groups (H1WB···O1C= 1.97 Å, O1W–H1WB···O1C= 169°, symmetry code: C = -*x*+1, *y*-1/2, -*z*+1/2) to form a 3D supramolecular framework. If these hydrogen bonds are taken into account, the 3D supramolecular framework of **4** shows a rare binodal (3,5)-connected **seh**-3,5-P21/c topology with the Schläfli symbol $(4.6^2)(4.6^7.8^2)$ (Fig. 4c). **4** possesses a solvent-accessible volume in the channels of about 156.2 $Å^3$ in the unit cell, which accounts for 5.2% of the total cell volume, as calculated by the PLATON program[17].

(Insert Fig. 4)

Effect of organic ligands on the structures of the MOFs

In this work, we selected three flexible bis(5,6-dimethylbenzimidazole) ligands and two different aromatic dicarboxylates to construct four target cobalt(II) complexes, aiming at examining the effect of aromatic carboxylates and the spacer of the flexible organic ligands on the assembly and structures of the resulting products. In **1** and **2**, the flexible L1 ligands uniformly behave as bis-monodentate linkers to connect the Co centers, the $bpdc^{2-}$ ligands take on a bidentate bridging μ_2-η^1:η^1 coordination fashion which act as linkers in a 3-fold interpenetrating 4-connected 6^6-**dia** topology for **1**, and the $npht^{2-}$ ligands adopt a μ_2-η^1:η^2 bridging fashion acting connectors,

which leads to a 3D uninodal 3-connected **ThSi$_2$** framework for **2**. In complexes **1**, **3**, and **4,** all of these three flexible N-containing ligands present a μ_2-bridging coordination mode, but their spacers exhibit different bending and rotating ability, which lead to generating different non-bonding Co···Co distances through the bis(5,6-dimethylbenzimidazole) ligands (14.387(12) Å for **1**, 10.337(13) Å for **3**, 10.011(10) Å for **4**) and different dihedral angles (0° in **1**, 87.95(2)° in **3**, 87.16(6)° in **4**) between two benzimidazole rings in a entire bis(5,6-dimethylbenzimidazole) ligand. Although the three Co(II) compounds involve the same dicarboxylic acid (H_2bpdc) secondary ligand, the coordination mode of bpdc^{2-} anions are different (μ_2-η^1:η^1, μ_2-η^2:η^2 and μ_2-η^1:η^2 mode in compounds **1**, **3**, **4**, respectively). Thus, the cobalt atoms are connected by bpdc^{2-} ligands and different flexible bis(5,6-dimethylbenzimidazole) ligands to generate a 3D **dia** array for **1**, a 2D uninodal 3-connected **hcb** layer with a point symbol of (6^3) for **3**, and a 2D **sql** topology with ($4^4.6^2$) for **4**, which is further extended into a 3D supramolecular framework by hydrogen bond interactions. It can be observed that the spacer of the flexible bis(5,6-dimethylbenzimidazole) ligands and carboxylate anions have a great influence on the construction of different structures in the self-assembly process of bis(5,6-dimethylbenzimidazole) polymers. The results further confirm that the subtle difference in organic ligand has a great influence on the architecture of multidimensional frameworks.

FT-IR spectra

The IR spectra exhibit the main characteristic bands of N-containing organic ligands, water molecules and carboxylate ligands for the title complexes (Fig. S1). There is no absorption peak around 1700 cm^{-1} for –COOH observed, indicating that all carboxyl groups of the organic moieties are deprotonated.[18] For the four complexes, the absorption peaks in the range of 1340-1670 cm^{-1} can be attributed to the asymmetric and symmetric vibrations of the carboxylate groups. Characteristic bands at 1524 cm^{-1} for **1**, 1534 cm^{-1} for **2**, 1515 cm^{-1} for **3** and 1554 cm^{-1} for **4** are assigned to the $\nu_{C=N}$ stretching vibration of the benzimidazole rings. The strong broad band, with its center around 3450 cm^{-1} for **2** and **4**, relates to the O–H stretching vibration modes of hydrogen bonds. Some weak bands at 2400-3100 cm^{-1} are consistent with the ν_{C-H} stretching vibration of the benzimidazole rings.

Thermal analysis and XRPD results

To evaluate the stability of the coordination architectures, thermogravimetric analyses (TGA) of

complexes **1**-**4** were performed (Fig. S2). The results show that complexes **1**-**4** are very stable in air at ambient temperature. There is only one weight loss stage in **1** or **3** and the weight loss corresponding to the release of the organic components is observed from 320 to 635 °C and 385 to 563 °C, for **1** and **3**, respectively. Finally, the remnants are 11.41% for **1** and 10.52% for **3**, which should be CoO (both of them calcd. 10.80%). Complexes **2** and **4** possess a two-step weight-loss process. For complex **2**, the weight loss of 2.11% in the first step from 90 to 158 °C corresponds to the removal of lattice water molecules. The TGA curve of **4** shows that the first weight loss of 1.93% between 156 and 183 °C corresponds to the loss of coordinated water molecule units (calcd. 2.89%). The second step with a weight-loss occurred in a temperature range from 255 to 648 °C for **2** and 329 to 485 °C for **3**, respectively, corresponding to the decomposition of the organic ligands. The remaining residue is attributed to the generation of CoO (obsd 11.61%, calcd 10.86% for **2**; obsd 12.06%, calcd 12.91% for **4**).

The phase purity of bulk materials was confirmed by XRPD experiments at room temperature. The XRPD experimental and calculated patterns are shown in Fig. S3. The experimental patterns of **1**-**4** are in good agreement with the corresponding simulated ones, indicating that the bulk synthesized material and the as-grown crystals are homogeneous.

Fluorescence properties

The photoluminescent properties of complexes **1**-**4** as well as the free L1, L2 and L3 ligands have been investigated in the solid state at room temperature (Fig. 5). The free ligands L1, L2 and L3 exhibit emission peaks at 378 (λ_{ex} = 343 nm), 383(λ_{ex} = 330 nm), and 318 nm (λ_{ex} = 313 nm), respectively, which can probably be assigned to the $n\rightarrow\pi^*$ or $\pi\rightarrow\pi^*$ transitions.[19] The emission bands are centered at 416 nm for **1**, 395 nm for **2**, 380 nm for **3**, and 392 nm for **4**, when excited at 250 nm. The emission band of **3** is similar to the free L2 ligand, which is neither metal-to-ligand charge transfer (MLCT) nor ligand-to-metal charge transfer (LMCT) in nature.[20] Thus, the emission may be assigned to the transitions of N-donor ligands. For complexes **1**, **2**, and **4**, it is clear that a red-shifted (38 nm for **1**, 17 nm for **2**, 74 nm for **4**) emission band has been observed compared with the free L1 and L3 ligands and can be tentatively ascribed to the ligand-to-metal charge transfer with electrons being transferred from Co(II) to the unoccupied π^* orbitals of the benzimidazolyl groups.[21]

(Insert Fig. 5)

Catalytic degradation experiments

Fenton oxidation technologies utilize H_2O_2, which generates hydroxyl radicals that are very effective in degrading organic pollutants, but the uncatalyzed reaction rates are generally slow at ambient temperature, and activation of H_2O_2 is necessary to accelerate the process. Transition metal coordination polymers are potential candidates to catalyze the degradation of such organic pollutants in a Fenton-like process.

The specific surface areas of the solid complexes **1**, **2, 3, 4** are 0.912 m^2/g, 0.783 m^2/g, 0.852 m^2/g and 0.813 m^2/g, respectivelycalculated using the nitrogen adsorption isotherms, respectively. Its unit cell are small and it has a large bulk density of about 1.3~1.4 cm^3/g. The degradation of the Congo red azo dye by hydrogen peroxide, activated with the title complexes, was investigated according to the literature,[22] and the results are shown in Fig. 6a. In the control experiment the Congo red and H_2O_2 mixture was stable without any noteworthy change in the absorbance of the dye, even for a reaction time up to 130 min, and the degradation efficiency of Congo red was only 13%, which indicates that there is almost no reaction going on between the Congo red and H_2O_2. When complex **1** or **2** as heterogeneous catalyst was introduced to the experiment system, the degradation efficiency of Congo red ended up to 89 or 98% after 130 min, respectively. However, when complex **3** or **4** was introduced into the system, only about 56 or 52% of the dye was decolored, respectively. Since Co(Ⅱ) species may play a key role in these reactions, an equivalent amount of $CoCl_2$ as catalyst were investigated under the same conditions. This proved to have a catalytic effect, but with a lower overall degradation efficiency of 38% compared to complexes **1** -4.

A pseudo-first-order kinetic model has being used to describe the degradation rate of the Congo red azo dye, and a plot of $\ln(C_{A0}/C_A)$ versus time in Fig. 6b visually reveals the rate of the catalytic reaction. The value of the rate constant (k) for the control experiment is 0.0016, which is extremely slower than that using coordination polymers **1**, **2**, **3** or **4** (k_1 = 0.0297, k_2 = 0.0191, k_3 = 0.0102, k_4 = 0.0070) as catalyst. Specifically, the reaction rate of the reaction containing coordination polymer **1** is significantly higher than the others. The catalytic activity may originate from the open metal sites, reactive functional groups and host matrices or nano-metric reaction

cavities. Based on the experimental observations, the reaction mechanism involving free radical species can be proposed as follows:

$$Co^{\square} - MOF + H_2O_2 \rightarrow Co^{\square} - MOF + \bullet OH + OH^- \quad (1)$$

$$Co^{\square} - MOF + H_2O_2 \rightarrow HO_2\bullet + Co^{\square} - MOF + H^+ \quad (2)$$

$$\text{azo dye} + \bullet OH \rightarrow \text{oxidation products} \quad (3)$$

The recyclability of these MOFs were examined by circulating runs in the catalytic degradation of Congo red azo dye over H_2O_2 system. As observed in Fig. S3 and Table S2, the catalytic performance of the complexes remained almost unchanged after two recycles, indicating that these MOFs are very stable and can be reused for the dye degradation.

The different catalytic activities of the title complexes may be due to the distinct coordination environments around the metal centers.[23] Overall, all the title complexes show higher activity as catalysts to degrade the Congo red azo dye in a fenton-like process.

(Insert Fig. 6)

Conclusion

In conclusion, a family of Co(II) coordination polymers based on flexible bis(5,6-dimethylbenzimidazole) ligands has been successfully synthesized and characterized. The results demonstrate that the spacer length of flexible bis(5,6-dimethylbenzimidazole) ligands and carboxylate anions play an important role in construction of coordination polymers with diverse structural features and charming topologies. In addition, polymers **1-4**, especially **1**, show promising catalytic activities in the decomposition of the Congo red dye in a Fenton-like process.

Supporting Information Available: CCDC number: 1013903-1013906 for the complexes **1-4**. The data can be obtained free of charge via https://services.ccdc.cam.ac.uk/structure_deposit (or from the Cambridge Cryst allographic Data Centre, 12, Union Road, Cambridge CB21EZ, UK; fax: (44)1223-336-033(44); or deposit@ccdc .cam.ac.uk).

Acknowledgments

The project was supported by the National Natural Science Foundation of China (51474086) and the Hercules Foundation (project AUGE/11/029 "3D-SPACE: 3D Structural Platform Aiming for Chemical Excellence") for funding.

References

1 (a) M. O'Keeffe and O. M. Yaghi, *Chem. Rev.*, 2012, **112**, 675; (b) X. J. Kong, L. S. Long, Z. P. Zheng, R. B. Huang and L. S. Zheng, *Acc. Chem. Res.*, 2010, **43**, 201; (c) K. J. Gagnon, H. P. Perry and A. Clearfield, *Chem. Rev.*, 2012, **112**, 1034; (d) S. J. Liu, Y. B. Huang, Z. J. Lin, X. F. Li and R. Cao, *RSC Adv.*, 2013, **3**, 9279; (e) K. K. Bisht, Y. Rachuri, B. Parmar, E. Suresh, *RSC Adv.*, 2014, **4**, 7352; (f) J. G. Ding, C.Yin, L. Y. Zheng, S. S. Han, B. L. Li, B. Wu, *RSC Adv.*, 2014, **4**, 24594; (g) L. B. Sun, J. R. Li, J. Park, H. C. Zhou, *J. Am. Chem. Soc*. 2012, **134**, 126.

2 (a) T. R. Cook, Y. R. Zheng and P. J. Stang, *Chem. Rev*. 2013, **113**, 734; (b) G. H. Cui, C. H. He, C. H. Jiao, J. C. Geng and V. A. Blatov, *CrystEngComm*, 2012, **14**, 4210; (c) C. W. Hu, T. Sato, J. Zhang, S. Moriyama and M. Higuchi, *J. Mater. Chem. C*, 2013, **1**, 3408; (d) M. H. Zeng, Q. X. Wang, Y. X. Tan, S. Hu, H. X. Zhao, L. S. Long and M. Kurmoo, *J. Am. Chem. Soc.,* 2010, **132**, 2561.

3 (a) B. Zheng, J. Bai and Z. Zhang, *CrystEngComm*, 2010, **12**, 49; (b) Y. F. Zhou, B. Y. Lou, D. Q. Yuan, Y. Q. Xu, F. L. Jiang and M. C. Hong, *Inorg. Chim. Acta.*, 2005, **358**, 3057; (c) J. Yang, B. Wu, F. Zhuge, J. Liang, C. Jia, Y. Y. Wang, N. Tang, X. J. Yang and Q. Z. Shi, *Cryst. Growth Des.*, 2010, **10**, 2331.

4 (a) V. S. S. Kumar, F. C. Pigge and N. P. Rath, *New J. Chem.*, 2004, **28**, 1192; (b) X. X. Wang, Y. G. Liu, Y. H. Li and G. H. Cui, *Trans. Met. Chem*., 2014, **39**, 461; (c) Y. J. Qi, Y. H. Wang, C. W. Hu, M. H. Cao, L. Mao and E. B. Wang, *Inorg. Chem*., 2003, **42**, 8519; (d) S. L. Xiao, L. Qi, P. J. Ma and G. H. Cui. *Z. Anorg. Allg. Chem.*, 2013, **639**, 1855.

5 (a) C. Y. Xu, Q. Q. Guo, X. J. Wang, H. W. Hou and Y. T. Fan, *Cryst. Growth Des*., 2011, **11**, 1869; (b) C. L. Ming, H. Zhang, G. Y. Li, and G. H. Cui, *Bull. Korean Chem. Soc.*, 2014, **35**, 651; (c) L. Liu, Y. H. Liu, G. Han, D. Q. Wu, H. W. Hou and Y. T. Fan, *Inorg. Chim. Acta*, 2013, **403**, 25.

6 (a) X. L. Wang, L. L. Hou, J. W. Zhang, G. C. Liu and H. Y. Lin, *Polyhedron*, 2013, **61**, 65; (b) L. Qin, L. N. Wang, P. J. Ma and G. H. Cui, *J. Molec. Struct.*, 2014, **1059**, 202; (c) J. M. Hao, Y. H. Li, H. H. Li and G. H. Cui, *Trans. Met. Chem*., 2014, **39**, 1; (d) L. L. Liu, J. J. Huang, X. L. Wang, G. C. Liu, S. Yang and H. Y. Lin, *Inorg. Chim. Acta*, 2013, **394**, 715; (e) S. L. Xiao, Y. H. Li, P. J. Ma and G. H. Cui, *Inorg. Chem. Comm.*, 2013, **37**, 54; (f) X. L. Wang, S. Yang,

G. C. Liu, J. J. Huang and H. Y. Lin, *Polyhedron*, 2012, **52**, 448; (g) S. L. Xiao, L. Qin, P. J. Ma and G. H. Cui, *Z. Anorg. Allg. Chem.*, 2013, **639**, 1855; (h) L. Qin, L. W. Liu, X. Du and G. H. Cui, *Trans. Met. Chem*., 2013, **38**, 85; (i) S. L. Xiao, L. Qin, C. H. He, X. Du and G. H. Cui, *J. Inorg. Organomet. Polym.*, 2013, **23**, 771.

7 (a) C. Y. Xu, L. K. Li, Y. P. Wang, Q. Q Guo, X. J. Wang, H. W. Hou and Y. T. Fan, *Cryst. Growth Des*., 2011, **11**, 4667; (b) G. X. Liu, K. Zhu, H. M. Xu, S. Nishihara, R. Y. Huang and X. M. Ren, *CrystEngComm*, 2009, **11**, 2784; (c) S. L. Xiao, L. Qin, C. H. He, X. Du and G. H. Cui, *J. Inorg. Organomet. Polym.*, 2013, **23**, 771.

8 L. L. Li, H. X. Li, Z. G. Ren, D. Liu, Y. Chen, Y. Zhang and J. P. Lang, *Dalton Trans*., 2009, **40**, 8567.

9 G. M. Sheldrick, *SADABS*. University of Göttingen, Göttingen, Germany, 1996.

10 G. M. Sheldrick, *Acta. Cryst.*, 2008, **A64**, 112.

11 (a) C. P. Li, J. Chen and M. Du. *CrystEngComm*, 2010, **12**, 4392; (b) L. Qin, Y. H. Li, P. J. Ma and G. H. Cui, *J. Molec. Struct.*, 2013, **1051**, 215; (c) H. M. Li, J. M. Zhou, W. Shi, X. J. Zhang, Z. J. Zhang, M. Zhang and P. Cheng. *CrystEngComm*, 2014, **16**, 834.

12 L. Yang, D. R. Powell and R. P. Houser, *Dalton Trans.*, 2007, **9**, 955.

13 (a) J. C. Geng, C. J. Wang, F. Wang, H. R. Luo, C. C. Zhao and G. H. Cui, *Chin, J. Inorg. Chem.*, 2012, **28**, 1060; (b) N. Chen, P. Yang, X. He, M. Shao and M. X. Li, *Inorg. Chim. Acta*, 2013, **405**, 43.

14 (a) V. A. Blatov, *Struct. Chem.*, 2012, **23**, 955; (b) M. Li, D. Li, M. O'Keeffe and O. M. Yaghi, *Chem. Rev.*, 2014, **114**, 1343.

15 I. A. Baburin, V. A. Blatov, L. Carlucci, G. Ciani and D. M. Proserpio. *J. Solid State Chem.*, 2005, **178**, 2452.

16 V. A. Blatov, L. Carlucci, G. Ciani and D. M. Proserpio. *CrystEngComm*, 2004, **6**, 378.

17 (a) X. L, H. L. Sun, X. S. Wu, X. Qiu and M. Du. *Inorg. Chem*., 2010, **49**, 1865; (b) L. Liu, C. Huang, Z. C. Wang, D. Q. Wu, H. W. Hou and Y. T. Fan, *CrystEngComm*, 2013, **15**, 7095.

18 (a) X. J. Gu and D. F. Xue, *Cryst. Growth Des.*, 2006, **6**, 2551; (b) C. P. Li, J. Chen, Q. Yu and M. Du, *Cryst. Growth Des.*, 2010, **10**, 1623.

19 (a) H. Y. Bai, J. Yang, B. Liu, J. F. Ma, W. Q. Kan and Y. Y. Liu, *CrystEngComm* 2011, **13**, 5877; (b) X. Y. Huang, K. F. Yue, J. C. Jin, J. Q. Liu, C. J. Wang, Y. Y. Wang and Q. Z. Shi,

Inorg. Chem. Comm., 2010, **13**, 338.

20 (a) T. L. Hu, R. Q. Zou, J. R. Li and X. H. Bu, *Dalton Tra*ns., 2008, **20**, 1302; (b) L. F. Ma, Q. L. Meng, C. P. Li, B. Li, L. Y. Wang, M. Du and F. P. Liang, *Cryst. Growth Des.*, 2010, **10**, 3036; (c) L. F. Ma, C. P. Li, L. Y. Wang and M. Du, *Cryst. Growth Des.*, 2010, **10**, 2641.

21 (a) M. D. Allendorf, C. A. Bauer, R. K. Bhakta and R. J. T. Houk, *Chem. Soc. Rev.*, 2009, **38**, 1330; (b) Y. W. Li, H. Ma, Y. Q. Chen, K. H. He, Z. X. Li and X. H. Bu, *Cryst. Growth Des.*, 2012, **12**, 189; (c) H. Ren, T. Y. Song, J. N. Xu, S. B. Jing, Y. Yu, P. Zhang and L. R. Zhang, *Cryst. Growth Des.*, 2009, **9**, 105.

22 (a) J. C. Geng, L. Qin, C. H. He and G. H. Cui, *Trans. Met. Chem.*, 2012, **37**, 579; (b) V. S. Mane and P. V. Vijay Babu, *J. Taiwan Inst. Chem. Eng.*, 2013, **44**, 81.

23 (a) S. L. Xiao, Y. G. Liu, L. Qin and G. H. Cui, *Inorg. Chem. Commun.*, 2013, **36**, 220; (b) J. C. Geng, L. W. Liu, S. L. Xiao and G. H. Cui, *Trans. Met. Chem.*, 2013, **38**, 143.

Table 1 Crystallographic data and structure refinement details for complexes **1**-**4**

Complex	**1**	**2**	**3**	**4**
Empirical formula	$C_{40}H_{34}CoN_4O_4$	$C_{34}H_{32}CoN_5O_{7.50}$	$C_{40}H_{34}CoN_4O_4$	$C_{33}H_{30}CoN_4O_5$
Formula weight	693.64	689.58	693.64	621.54
Crystal system	Monoclinic	Monoclinic	Orthorhombic	Monoclinic
Space group	*C*2/*c*	*C*2/*c*	*pbca*	$P2_1/c$
a/Å	23.6808(19)	19.0540(3)	11.4409(12)	10.5449(11)
b/Å	13.9240(12)	16.0040(2)	24.6960(3)	9.9472(10)
c/Å	10.909(12)	21.248(3)	25.285(3)	28.910(3)
α/(°)	90	90	90	90
β/(°)	91.602(10)	100.471(2)	90	94.899(10)
γ/(°)	90	90	90	90
Volume/Å^3	3595.6(6)	6371.4(15)	7144.1(14)	3021.3(5)
Z	4	8	8	4
Calculated density/(g/cm^3)	1.281	1.438	1.290	1.366
F(000)	1444	2864	2888	1292
θ range/(°)	1.70 to 27.54	1.67 to 27.55	2.12 to 25.02	2.17 to 27.48
Reflections collected	10848	19225	52018	27229
Unique date	4091	7294	6304	6908
R_{int}	0.0415	0.0597	0.1422	0.1011
Data/restraint/parameters	4091/0/224	7294/48/455	6304/0/446	6908/0/392
GOF on F^2	1.017	0.906	0.883	0.997
Final *R* indices ($I > 2\sigma(I)$)	R1 = 0.0432 wR2 = 0.0980	R1 = 0.0572 wR2 = 0.1380	R1 = 0.0589 wR2 = 0.1667	R1 = 0.0533 wR2 = 0.1055
R indices (all data)	R1 = 0.0715 wR2 = 0.1117	R1 = 0.1196 wR2 = 0.1656	R1 = 0.1349 wR2 = 0.2342	R1 = 0.1226 wR2 = 0.1288
Largest diff. peak and hole	0.267, -0.320	0.475, -0.388	0.329, -0.308	0.482, -0.422

[a] $R_1 = \Sigma||F_o|-|F_c||/\Sigma|F_o|$; [b] $wR_2 = \{\Sigma [w (F_o^2-F_c^2)^2]/\Sigma [w (F_o^2)^2]\}^{1/2}$

Caption to Figures

Figure 1. (a) The coordination environment of Co(II) ion in **1**. Hydrogen atoms are omitted for clarity (30% ellipsoid probability). Symmetry codes: A, -*x*+1, *y*, -*z*+3/2; B, -*x*-3/2, -*y*-3/2, -*z*-1; C, *x*, -*y*, *z*+1/2; (b) View of the 3D framework of **1**. The green, blue, pink, orange nodes stand for Co, N, O, C atoms, respectively; (c) Schematic illustration of the three-fold interpenetrating network in **1**. All the nodes stand for Co atoms.

Figure 2. (a) The coordination environment of Co(II) ion in **2**. Hydrogen atoms are omitted for clarity (30% ellipsoid probability). Symmetry codes: A, -*x*+3/2, –*y*+3/2, -*z*+1; B, -*x*+1, *y*, -*z*+3/2; (b) The 1D mononuclear $[Co_2(npht)_2]$ unit in **2**; (c) View of the 3D framework of **2**. The green, blue, pink, orange nodes stand for Co, N, O, C atoms, respectively; (d) Corresponding 3-connected **$ThSi_2$** network for **2**. The blue nodes stand for 3-connected Co atoms.

Figure 3. (a) The coordination environment of Co(II) ion in **3**. Hydrogen atoms are omitted for clarity (30% ellipsoid probability). Symmetry codes: A, -*x*, -*y*+1, -*z*-1 B, -*x*+3/2, *y*+1/2, *z*; (b) View of the 2D grid layer for **3**. The green, blue, pink, orange nodes stand for Co, N, O, C atoms, respectively; (c) The uninodal 3-connected **hcb** topology for **3**. The pink nodes stand for 3-connected Co atoms.

Figure 4. (a) The coordination environment of Co(II) ion in **4**. Hydrogen atoms are omitted for clarity (30% ellipsoid probability). Symmetry codes: A, *x*, -*y*+3/2, *z*+1/2 B, -*x*+2, *y*-1/2, -*z*+1/2; (b) View of the 2D network for **4**. The green, blue, pink, orange nodes stand for Co, N, O, C atoms, respectively; (c) A schematic representation of the 3D supramolecular framework formed by H-bonds with binodal (3,5)-connected **seh**-3,5-P21/c topology. The dashed, green and pink nodes represent hydrogen bond, 5-connected Co atoms and 3-connected $bpdc^{2-}$ ligands, respectively.

Figure 5. (a) Emission spectra of **1**, **2** and free L1 ligand in the solid state at room temperature; (b) Emission spectra of **3**, **4** and free L2, L3 ligands in the solid state at room temperature.

Figure 6. (a) The experiment results of the catalytic degradation of Congo red; (b) Plot of $\ln(C_{A0}/C_A)$ as a function of time for selected initial dye concentrations assuming the reaction is a pseudo-first order with respect to Congo red.

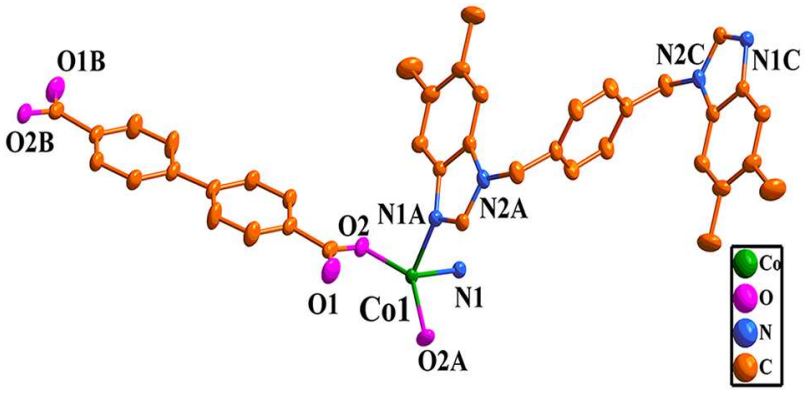

(a)

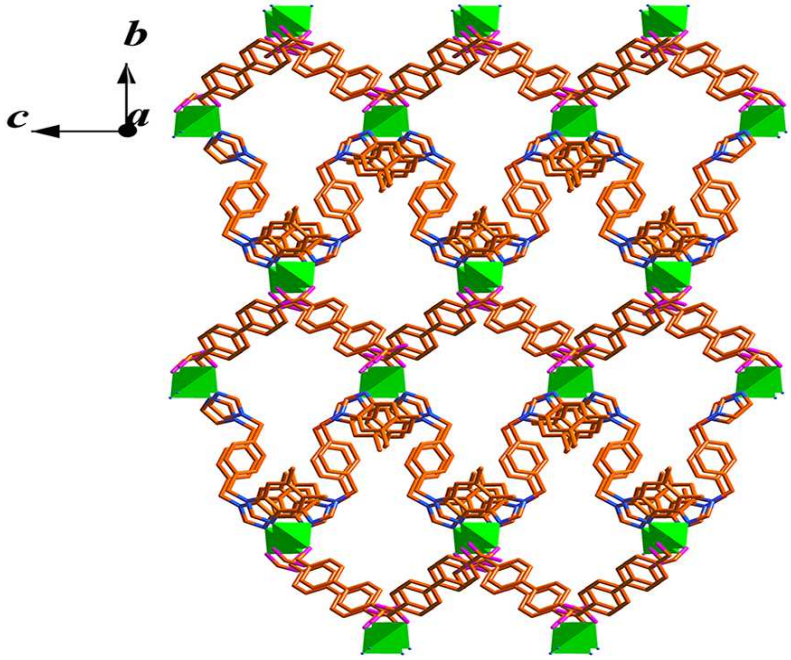

(b)

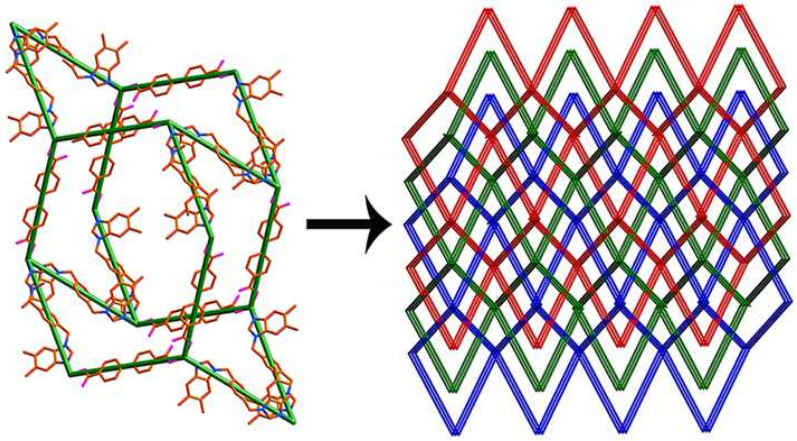

(c)

Figure 1

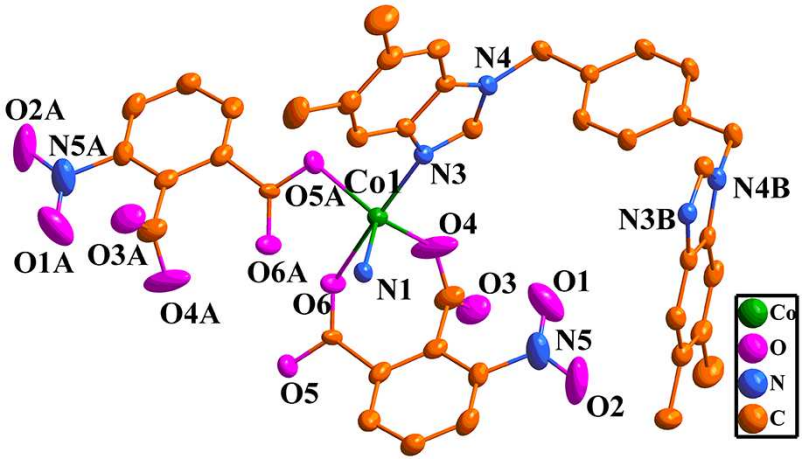

(a)

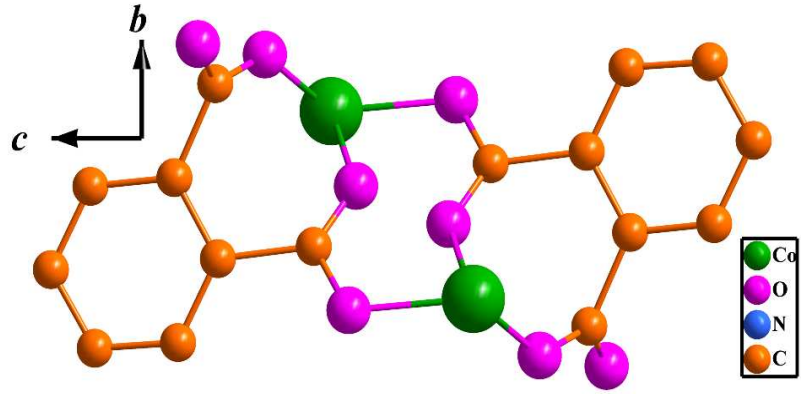

(b)

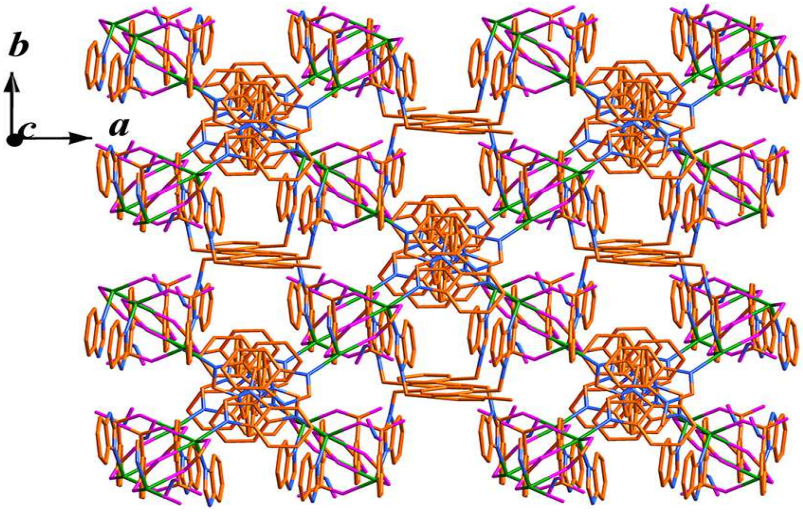

(c)

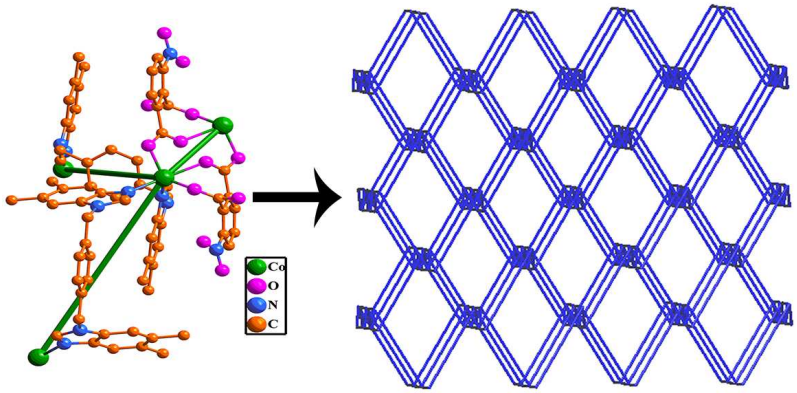

(d)

Figure 2

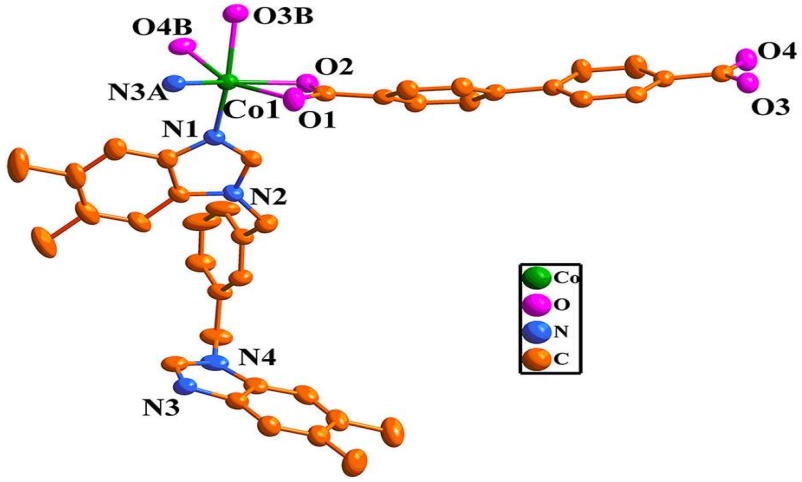

(a)

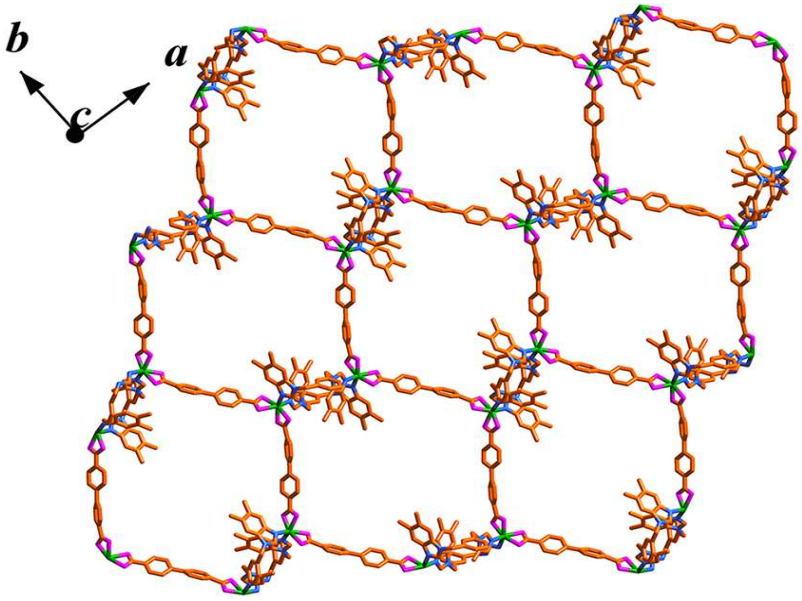

(b)

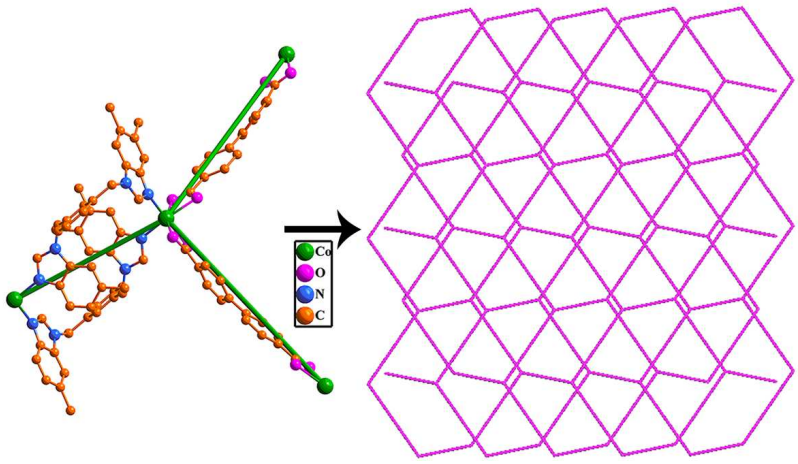

(c)

Figure 3

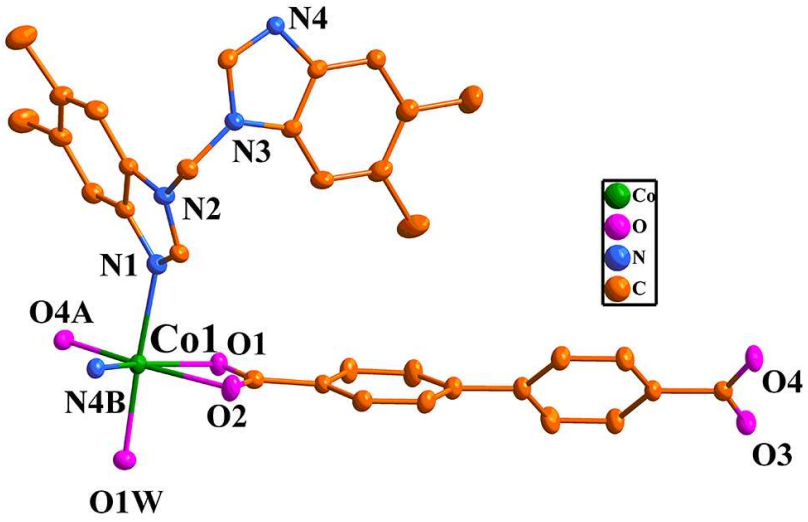

(a)

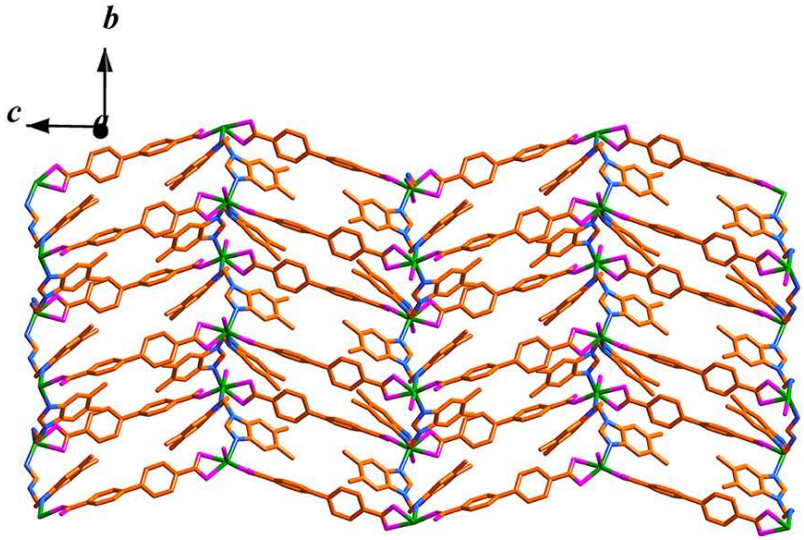

(b)

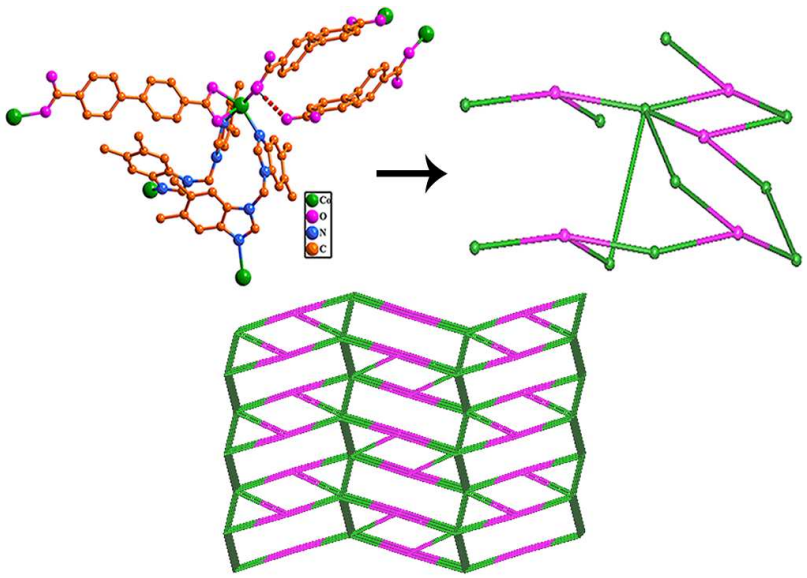

(c)

Figure 4

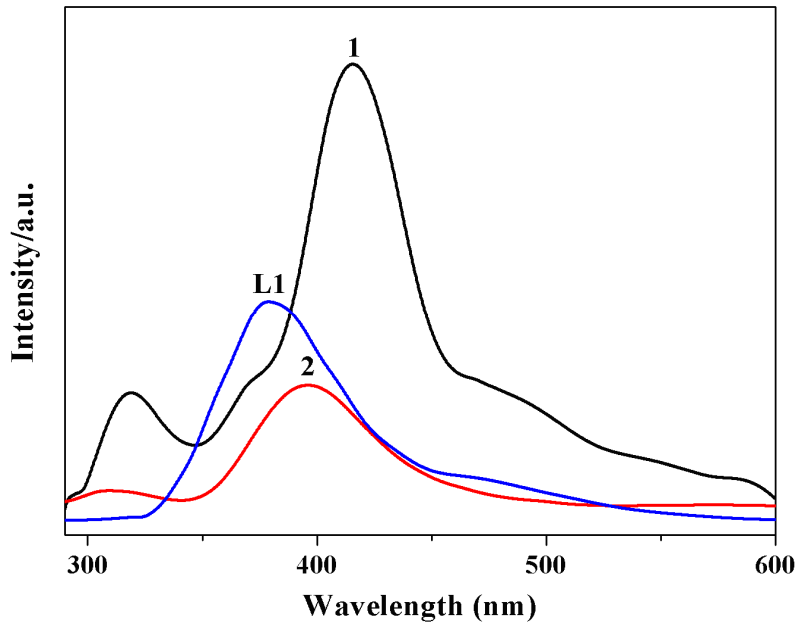

(a)

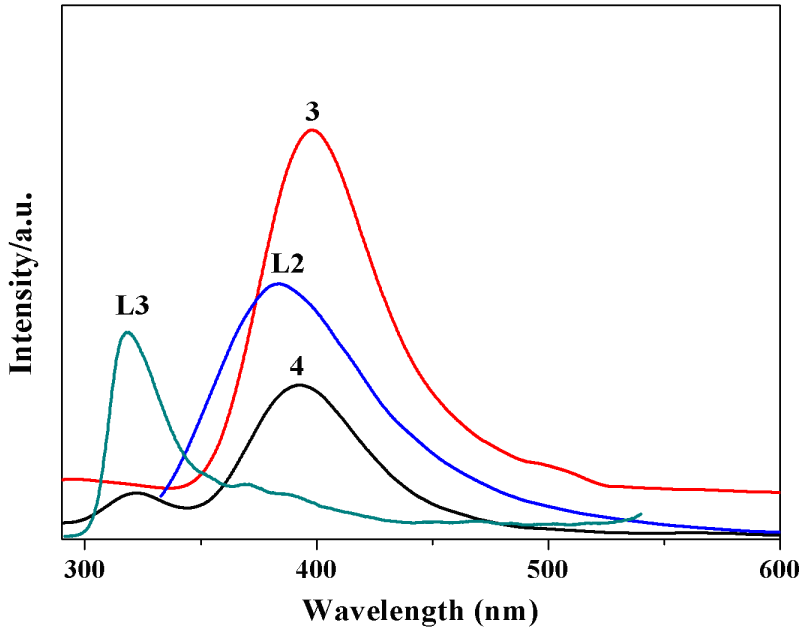

(b)

Figure 5

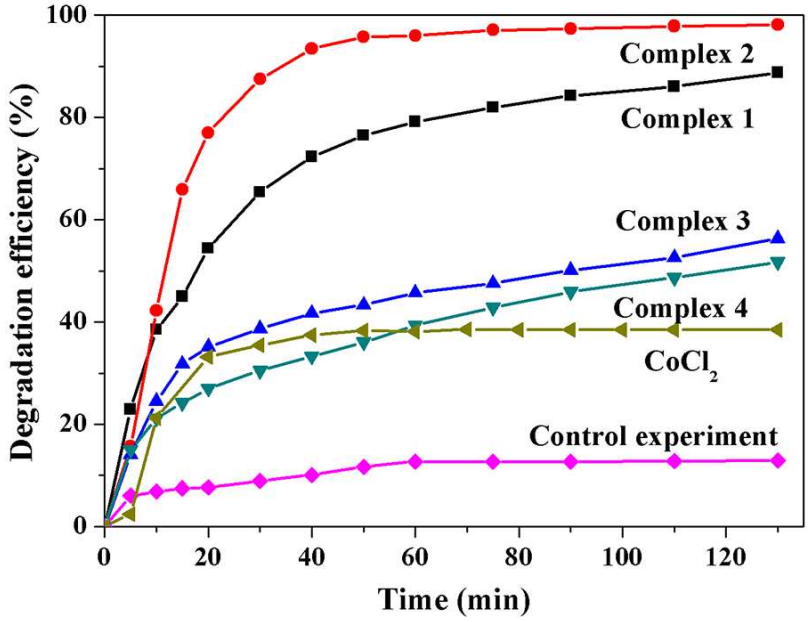

(a)

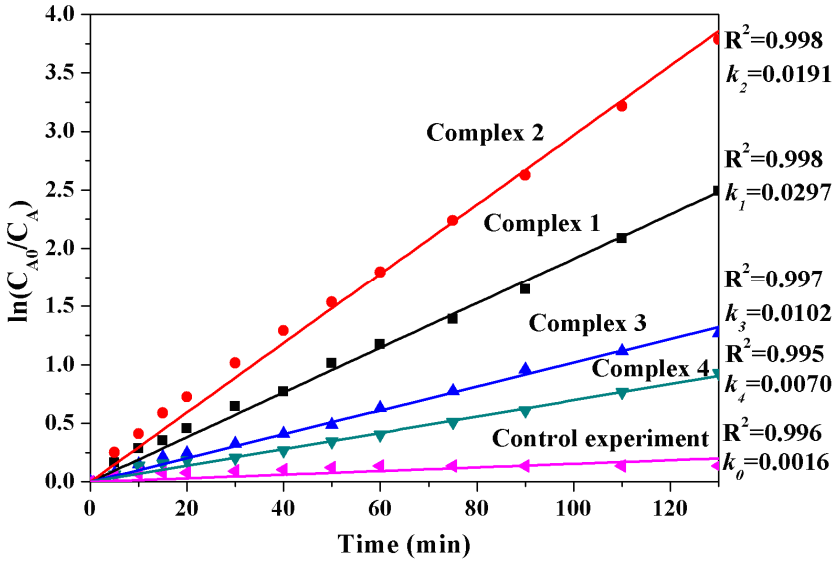

(b)

Figure 6

Synopsis

Four cobalt(II) coordination polymers with diverse topologies derived from flexible bis(benzimidazole) and aromatic dicarboxylic acids：Syntheses, crystal structures and catalytic properties

Xiao Xiao Wang[a], Baoyi Yu[b], Kristof Van Hecke[b], Guang Hua Cui*[a]

[a]*College of Chemical Engineering, Hebei United University, 46 West Xinhua Road, Tangshan 063009, Hebei, PR China.*

[b]*Department of Inorganic and Physical Chemistry, Ghent University, Krijgslaan 281 S3, B-9000 Ghent, Belgium*

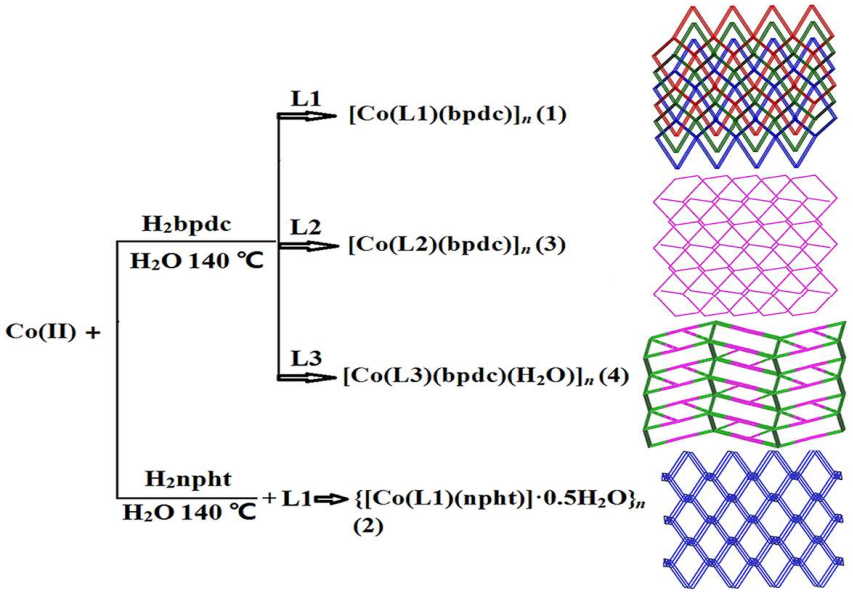

Four metal-organic frameworks (MOFs) were obtained from the hydrothermal reaction of Co(II) and with dicarboxylic acid and flexible bis(5,6-dimethybenzimidazole) and characterized. The four MOFs exhibit distinct 2D or 3D structural frameworks. These results demonstrate that the spacer length of flexible bis(5,6-dimethylbenzimidazole) ligands and carboxylate anions play an important role in construction of coordination polymers with diverse structural features and charming topologies.